

# Dual Emissive Multinuclear Iridium(III) Complexes in Solutions: Linear Photophysical Properties, Two-Photon Absorption Spectra, and Photostability

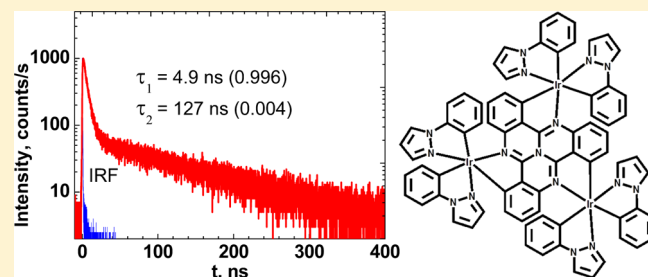
Peng Zhao,<sup>†</sup> Salimeh Tofighi,<sup>†</sup> Ryan M. O'Donnell,<sup>‡</sup> Jianmin Shi,<sup>‡</sup> Mykhailo V. Bondar,<sup>\*,†,§</sup> David J. Hagan,<sup>†</sup> and Eric W. Van Stryland<sup>\*,†</sup>

<sup>†</sup>CREOL, College of Optics and Photonics, University of Central Florida, Orlando, Florida 32816, United States

<sup>‡</sup>US Army Research Laboratory, Adelphi, Maryland 20783, United States

<sup>§</sup>Institute of Physics NASU, Prospect Nauki, 46, Kiev-28, Kyiv 03028, Ukraine

**ABSTRACT:** Linear steady-state and time-resolved spectroscopic properties, degenerate two-photon absorption (2PA) spectra, and photochemical stability of Ir<sup>III</sup> complexes TCQ[Ir<sup>III</sup>(ppz)<sub>2</sub>]<sub>n</sub> (TCQ = tricycloquinazoline; ppz = 1-phenylpyrazole; n = 1 (1), n = 2 (2), and n = 3 (3)) are presented for liquid solutions. The analysis of the linear photophysical properties revealed the nature of the observed dual-component fluorescence–phosphorescence emission of 1–3 at room temperature. The values of 2PA cross sections were determined by open aperture Z-scans using a 1 kHz femtosecond laser system. The specific dependence of the 2PA efficiency on the number of ppz ligand units in 1–3 was determined. The quantum yields, Φ<sub>ph</sub>, for photochemical decomposition of TCQ[Ir<sup>III</sup>(ppz)<sub>2</sub>]<sub>n</sub> complexes were obtained for the first time using the absorption method [Cui, L.-S.; et al. *ACS Appl. Mater. Interfaces* **2015**, *7*, 11007–11014] with continuous wave laser irradiation, and the highest stability of Φ<sub>ph</sub> ≈ 4 × 10<sup>-6</sup> was shown for 2 in toluene.



## INTRODUCTION

Investigations of the linear spectroscopic and nonlinear optical properties of metal–organic complexes is the subject of great interest for multiple practical applications, including organic electronics,<sup>1–5</sup> luminescence sensing,<sup>6–8</sup> bioimaging,<sup>9–11</sup> photodynamic therapy,<sup>12–14</sup> nonlinear optics,<sup>15–17</sup> etc. Iridium complexes with specific ligand compounds<sup>18–21</sup> are among the most promising structures for these applications because they exhibit extremely fast singlet–triplet conversion processes,<sup>22–25</sup> high intersystem crossing quantum yields,<sup>26–28</sup> and photochemical stability.<sup>29,30</sup> Ir complexes can exhibit efficient room-temperature phosphorescence,<sup>31,32</sup> good potential for color tunability,<sup>33–35</sup> and specific intramolecular charge-transfer processes, allowing noticeable enhancement in a broad variety of nonlinear optical interactions.<sup>8,36</sup> Ultrafast relaxation processes in the excited state of iridium compounds, including transient excited-state absorption kinetics, the rates of singlet–triplet conversion, and electronic structures of excited-state potential surfaces, were investigated for numerous molecular complexes, such as Ir(ppy)<sub>3</sub> (ppy = 2-phenylpyridine), Ir(DBQ)<sub>2</sub>(acac) (DBQ = dibenzo[*f,h*]quinoxaline; acac = acetylacetonate) and Ir(MDQ)<sub>2</sub>(acac) (MDQ = 2-methyl-dibenzo[*f,h*]quinoxaline),<sup>22</sup> bis-heteroleptic Ir complexes with ethynyltolyl, ethynylpyrene and ethynylperylene,<sup>24</sup> Ir(piq)<sub>3</sub> (piq = 1-phenylisoquinoline),<sup>23</sup> etc. The nature of the extremely rapid population (~10<sup>-13</sup> s) of the metal-to-ligand charge-transfer triplet electronic state (<sup>3</sup>MLCT) was revealed

for these complexes by femtosecond transient absorption spectroscopy.<sup>22,23</sup> Time-resolved dual emission processes in Ir complexes in solutions were previously reported in refs 19, 37 and characteristic luminescence peculiarities were explained by the double minima excited-state potential energy surface. The investigations of the molecular photochemical stability of metal–organic compounds are rarely presented, and those that are presented mainly concern relative measurements of the temporal changes in the absorption or luminescence spectra, i.e., the rates of photodecomposition occurring under photoexcitation as compared with reference objects.<sup>38–41</sup> The results of these types of measurements are strictly dependent on the employed experimental conditions and, in general, cannot serve as molecular characteristics of photostability, such as the photochemical decomposition quantum yield, Φ<sub>ph</sub>. It should be mentioned that the determination of values of Φ<sub>ph</sub> allow correct comparisons of the photostability for different molecular structures.<sup>42</sup>

Here, we continue linear spectroscopic and nonlinear optical investigations of these new Ir<sup>III</sup> complexes with tricycloquinazoline TCQ[Ir<sup>III</sup>(ppz)<sub>2</sub>]<sub>n</sub> (TCQ = tricycloquinazoline; ppz = 1-phenylpyrazole; n = 1 (1), n = 2 (2), and n = 3 (3)) in liquid solutions at room temperature, including the steady-state and

**Received:** December 22, 2017

**Revised:** February 14, 2018

**Published:** February 16, 2018

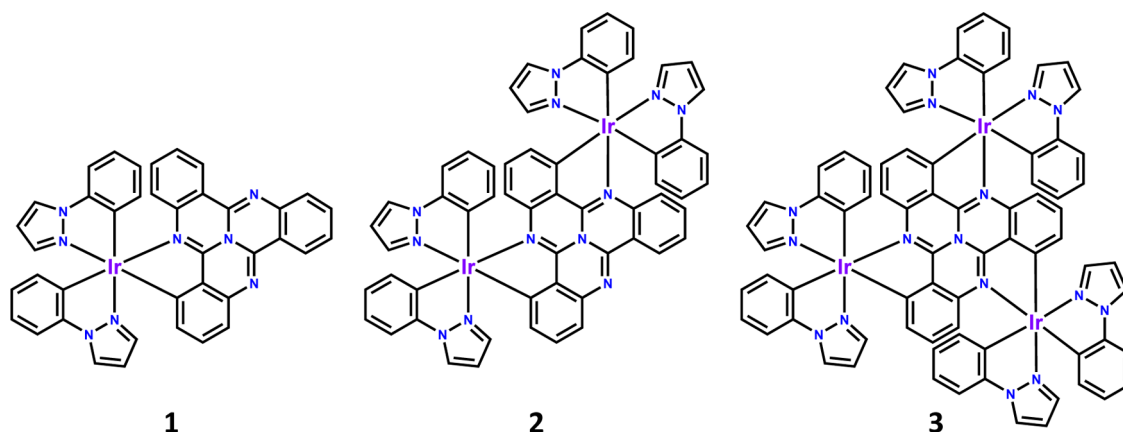


Figure 1. Molecular structures of iridium complexes 1–3.

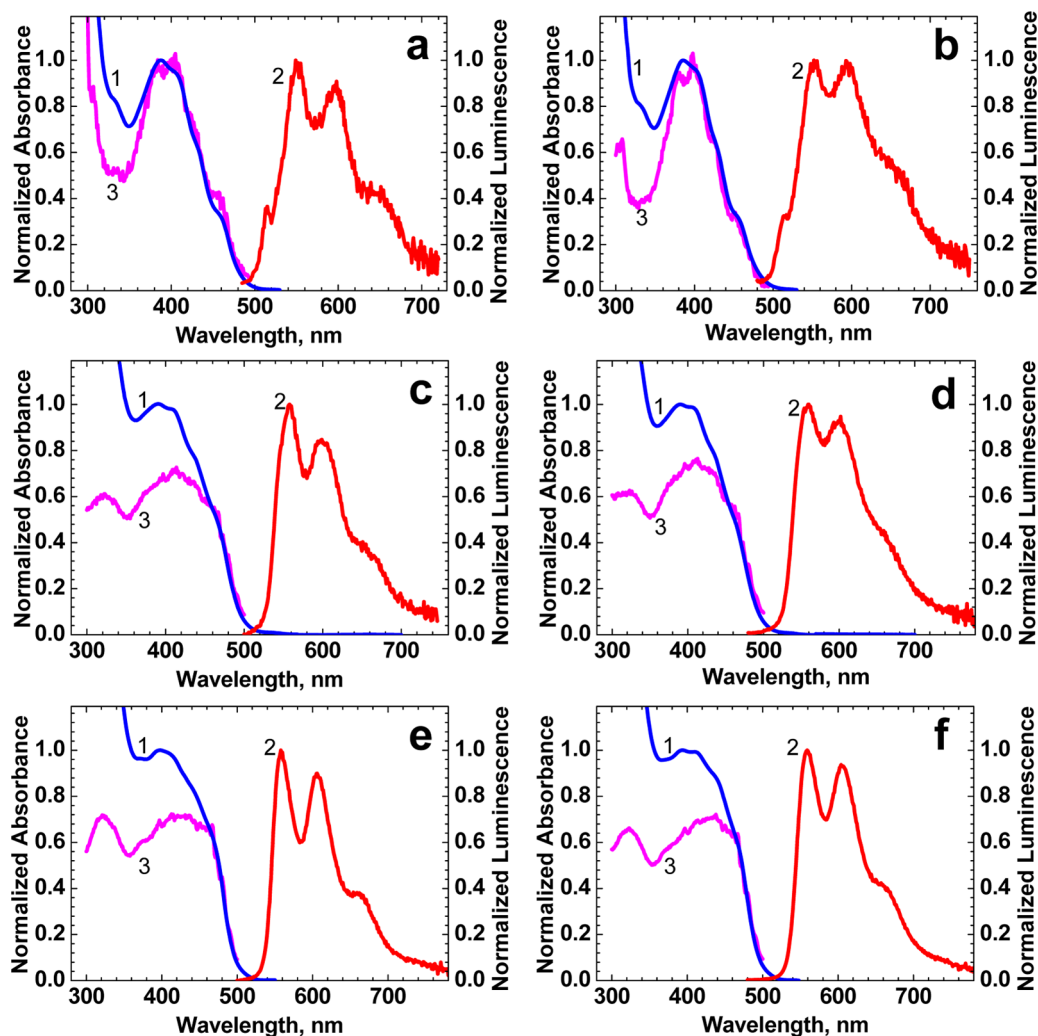


Figure 2. Normalized IPA (1), PL emission (2), and excitation (3) spectra of iridium complexes 1 (a, b), 2 (c, d), and 3 (e, f) in different solvents, i.e., TOL (a, c, e) and DCM (b, d, f). The excitation spectra are observed at a wavelength of  $\lambda_{\text{obs}} = 560$  nm.

73 time-resolved luminescence properties, the analysis of the  
74 observed dual-component fluorescence–phosphorescence  
75 emission and corresponding nature of the excited-state  
76 electronic structures, two-photon absorption (2PA) spectra,  
77 and photodecomposition quantum yields.

78 It should be mentioned that the synthesis of 1–3, their  
79 transient absorption spectra, triplet–triplet absorption cross

sections, and nano- and picosecond Z-scan measurements at  
532 nm were reported in the previous work.<sup>16</sup> The new set of  
data obtained here allows deeper understanding of the nature of  
the electronic structures of 1–3 and completes the  
experimental characterization of new TCQ[Ir<sup>III</sup>(ppz)<sub>2</sub>]<sub>n</sub> com-  
plexes, which can be useful for practical applications in 85

Table 1. Photophysical Parameters of 1–3 in Liquid Solutions at Room Temperature<sup>a</sup>

N/N	1		2		3	
solvent	TOL	DCM	TOL	DCM	TOL	DCM
$\lambda_{ab}^{max}$ , nm	388 ± 1	386 ± 1	390 ± 1	390 ± 1	398 ± 1	396 ± 1
$\lambda_{PL}^{max}$ , nm	551 ± 2	553 ± 2	558 ± 2	558 ± 2	559 ± 2	560 ± 2
Stokes shift, nm	163 ± 2	167 ± 2	168 ± 2	168 ± 2	161 ± 2	164 ± 2
(cm <sup>-1</sup> )	(7620)	(7820)	(7720)	(7720)	(7240)	(7400)
$\epsilon^{max} \times 10^{-3}$ , M <sup>-1</sup> cm <sup>-1</sup>	20 ± 2 (388)	22 ± 2 (386)	20.4 ± 2 (390)	21.2 ± 2 (389)	23.6 ± 2 (398)	22.8 ± 2 (395)
$\Phi_{PL}^b$	0.0027 ± 0.0015	0.0033 ± 0.0015	0.004 ± 0.0015	0.0066 ± 0.002	0.02 ± 0.005	0.03 ± 0.005
$\tau$ , ns	4.9 (0.996)	4.8 (0.999)	4.9 (0.94)	4.7 (0.992)	156 ± 1	5.2 (0.92)
(A <sub>1</sub> ) <sup>c</sup>	127 (0.004)	>370 (0.001)	148 (0.06)	356 (0.008)		398 (0.08)
$\Phi_{ph} \times 10^6$	5 ± 1	10 ± 2	4 ± 0.8	16 ± 3	5 ± 3	20 ± 4

<sup>a</sup>Absorption  $\lambda_{ab}^{max}$  and luminescence  $\lambda_{PL}^{max}$  maxima, Stokes shifts, extinction coefficients  $\epsilon^{max}$  ( $\lambda_{ab}^{max}$ ), PL emission quantum yields  $\Phi_{PL}$ , PL lifetimes  $\tau$ , and photodecomposition quantum yields  $\Phi_{ph}$ . <sup>b</sup>Obtained under excitation at 373 nm. <sup>c</sup>Normalized amplitudes of the corresponding lifetime components (lifetimes are obtained for air-saturated solutions).

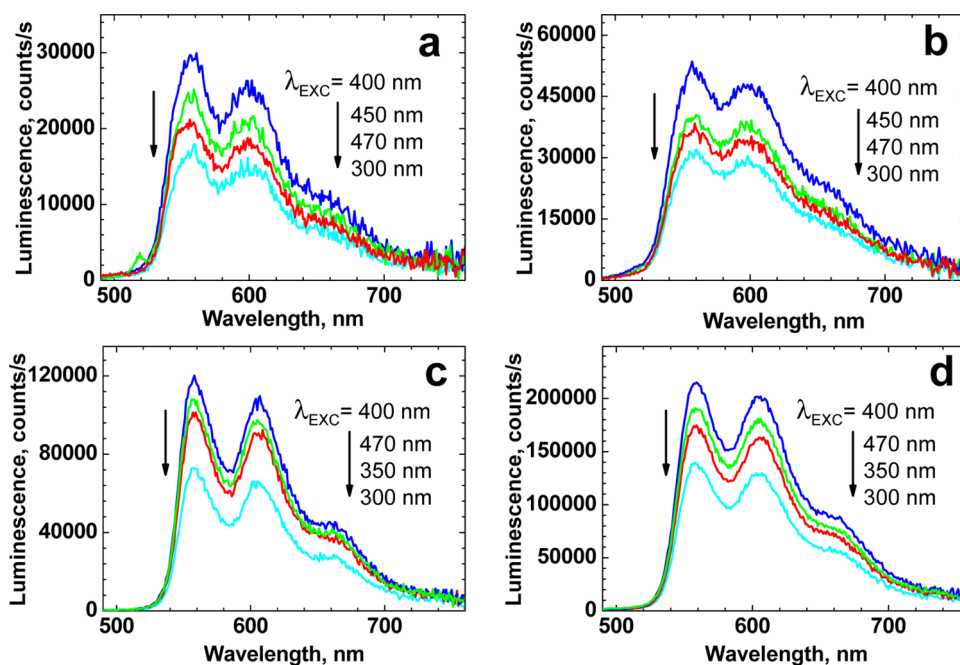


Figure 3. Steady-state PL spectra of 2 (a, b) and 3 (c, d) in TOL (a, c) and DCM (b, d) for the selected excitation wavelength,  $\lambda_{ex}$ .

86 luminescence sensing, organic photovoltaics, nonlinear optics,  
87 etc.

## 88 ■ EXPERIMENTAL SECTION

89 **Linear Spectroscopic and Photochemical Measure-**  
90 **ments.** The chemical structures of the investigated compounds  
91 1–3 are designed, synthesized at U.S. Army Research  
92 Laboratory,<sup>16,43</sup> and presented in Figure 1. These complexes  
93 are not planar as each iridium center exhibits an octahedral  
94 geometry with respect to the attached ligands. As such, no  
95 electronic communication is expected to occur between the  
96 individual ligands. All linear photophysical and photochemical  
97 parameters of 1–3 were obtained at room temperature in  
98 spectroscopic grade.

99 Toluene (TOL) and dichloromethane (DCM) purchased  
100 from commercial suppliers and used without further  
101 purification. The steady-state linear one-photon absorption  
102 (1PA) spectra were recorded on a Varian CARY-500  
103 spectrophotometer using 10 mm path length quartz cuvettes  
104 with solute concentrations  $C \sim (2-5) \times 10^{-5}$  M. The steady-  
105 state corrected luminescence and excitation spectra and

emission lifetimes were measured with a FLS980 spectro-  
106 fluorometer (Edinburgh Instruments Ltd.) using 10 mm path  
107 length spectrofluorometric quartz cuvettes and dilute solutions  
108 ( $C \sim (1-2) \times 10^{-6}$  M). The photoluminescence (PL)  
109 quantum yields,  $\Phi_{PL}$ , of the Ir<sup>III</sup> complexes were determined  
110 by the relative method<sup>44</sup> using dilute solution of 9,10-  
111 diphenylanthracene in cyclohexane as a reference ( $\Phi_{PL} =$   
112 0.95).<sup>45</sup> Photochemical properties of 1–3 in the employed  
113 solvents were investigated under linear excitation with a  
114 continuous wave (CW) diode laser (excitation wavelength,  
115  $\lambda_{ex} \approx 405$  nm and average irradiance  $I(\lambda_{ex}) \approx 300$  mW cm<sup>-2</sup>).  
116 The photochemical decomposition quantum yields,  $\Phi_{ph}$ , were  
117 obtained from absorption measurements as<sup>46</sup> 118

$$\Phi_{ph} = \frac{[D(\lambda, 0) - D(\lambda, t_{ir})] \cdot N_A}{10^3 \cdot \epsilon(\lambda) \cdot I(\lambda) \cdot \int_0^{t_{ir}} [1 - 10^{-D(\lambda, t)}] dt}$$

where  $D(\lambda, t)$ ,  $N_A$ ,  $\epsilon(\lambda)$ ,  $I(\lambda)$ , and  $t_{ir}$  are the optical density of  
119 the solution at wavelength  $\lambda$  and time  $t$ , Avogadro's number,  
120 extinction coefficient (in M<sup>-1</sup> cm<sup>-1</sup>), laser irradiance (in  
121 photon cm<sup>-2</sup> s<sup>-1</sup>), and irradiation time, respectively. A 122

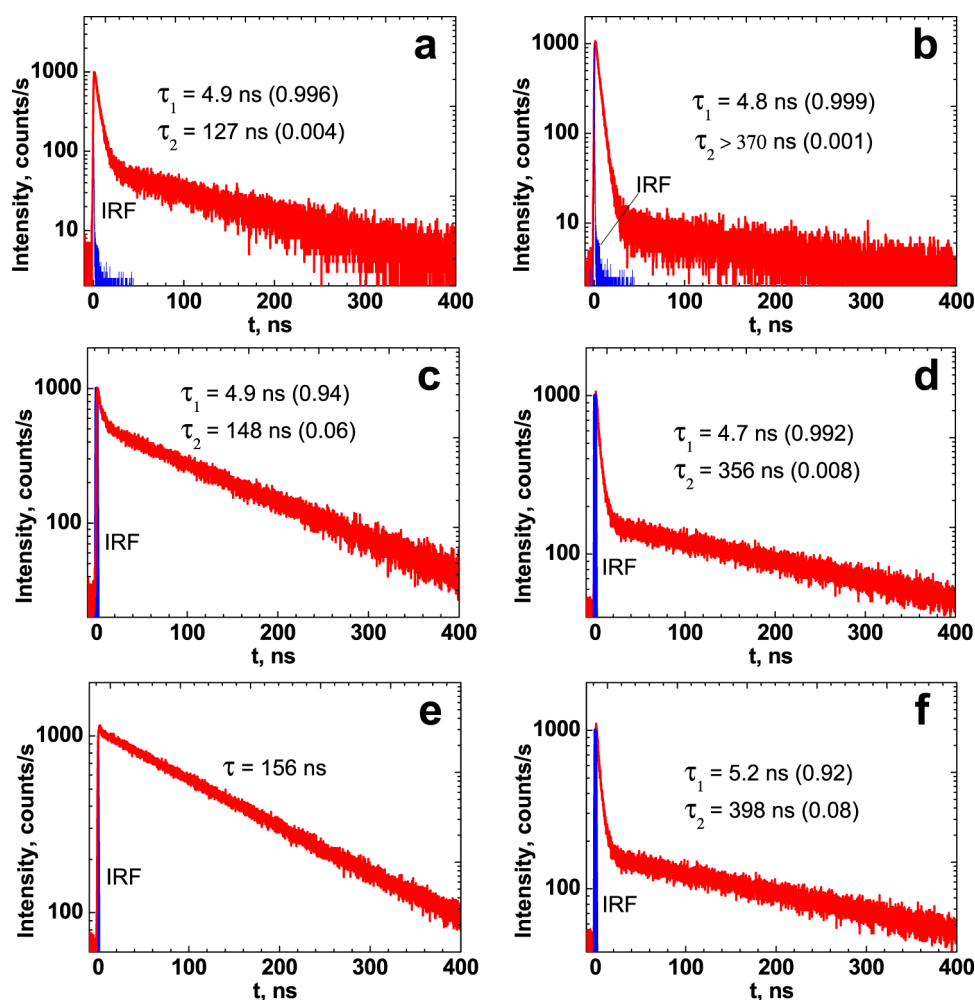


**Figure 4.** PL decay curves (marked in red) of iridium complexes **1** (a, b), **2** (c, d), and **3** (e, f) measured in TOL (a, c, e) and DCM (b, d, f) at the observation wavelength of  $\lambda_{\text{obs}} = 630$  nm.  $\tau$  is the time constant from an exponential decay fit. The instrument response function is marked in blue.

123 comprehensive description of the absorption method was  
124 described previously.<sup>46–48</sup>

125 **Two-Photon Absorption Cross-Sectional Measure-**  
126 **ments.** The degenerate 2PA spectra of **1–3** were obtained  
127 in DCM by a single-beam Z-scan method<sup>49</sup> using a commercial  
128 1 kHz femtosecond laser system (Ti:sapphire regenerative  
129 amplifier Legend Duo+, Coherent, Inc.)-pumped optical  
130 parametric amplifier (OPA) HE-TOPAS (Light Conversion,  
131 Inc.), with a tuning range  $\approx 1200$ – $2500$  nm. The frequency of  
132 the output beam from the OPA was doubled by a 1 mm barium  
133 borate crystal and sequentially filtered by multiple spike filters  
134 (full width at half-maximum  $\approx 10$  nm). The resulting output  
135 pulse duration was  $\approx 100$  fs and pulse energy was  $\leq 40$   $\mu\text{J}$ . The  
136 experimental Z-scan setup was calibrated for every wavelength  
137 with  $\text{SiO}_2$ ,  $\text{ZnSe}$ , and  $\text{CdSe}$  standards.<sup>50</sup>

## 138 ■ RESULTS AND DISCUSSION

139 **Linear Photophysical and Photochemical Properties**  
140 **of 1–3.** The steady-state IPA-corrected PL and excitation  
141 spectra along with the main photophysical and photochemical  
142 parameters of **1–3** are presented in Figure 2 and Table 1,  
143 respectively. The main long-wavelength IPA bands of **1–3** with  
144 maxima at  $\approx 390$ – $400$  nm exhibit a weak dependence on  
145 solvent polarity and, presumably, are related to the TCQ  
146 ligand-centered (LC)  $^1\pi\text{-}\pi^*$  transition<sup>51,52</sup> that strongly

147 overlaps with the manifold of other spin-allowed metal-to-  
148 ligand charge transfer  $S_0 \rightarrow ^1\text{MLCT}$  and very weak spin-  
149 forbidden  $S_0 \rightarrow ^3\text{MLCT}$  electronic transitions<sup>1,2,4</sup> ( $S_0$  is the  
150 ground electronic state of **1–3**). Comparing the short-  
151 wavelength parts of the absorption contours (Figure 2, curves  
152 1) and noting the close values of the maxima extinction  
153 coefficients  $\epsilon^{\text{max}}$  of **1–3** (see Table 1) along with the  
154 corresponding spectral data in refs 53, 54 allow us to conclude  
155 that the contributions of the (ppz)<sub>2</sub>-ligand-based electronic  
156 transitions into the main IPA bands are noticeably weaker than  
157 the contributions of the TCQ-based ones. The shapes and  
158 spectral positions of the steady-state PL spectra are nearly  
159 independent of  $\lambda_{\text{ex}}$  (Figure 3) in contrast to the PL emission  
160 quantum yields,  $\Phi_{\text{PL}}$ , which exhibit a large decrease under  
161 excitation in the short-wavelength spectral range in accordance  
162 with a strong deviation between IPA and the corresponding  
163 excitation spectra (see Figure 2, curves 1 and 3). This implies a  
164 complicated nature of the excited-state potential energy  
165 surfaces for iridium compounds **1–3**, resulting in the possibility  
166 of direct transitions from the higher excited electronic states to  
167  $S_0$ . The absolute values of  $\Phi_{\text{PL}}$  are relatively low,  $\leq 0.03$ , and  
168 increase in line with the number of iridium nuclei in the  
169 molecular structure (see data in Table 1). All of the investigated  
170 complexes exhibit double-exponential emission decay kinetics  
171 (Figure 4) except for **3** in nonpolar TOL where the short 171 f4

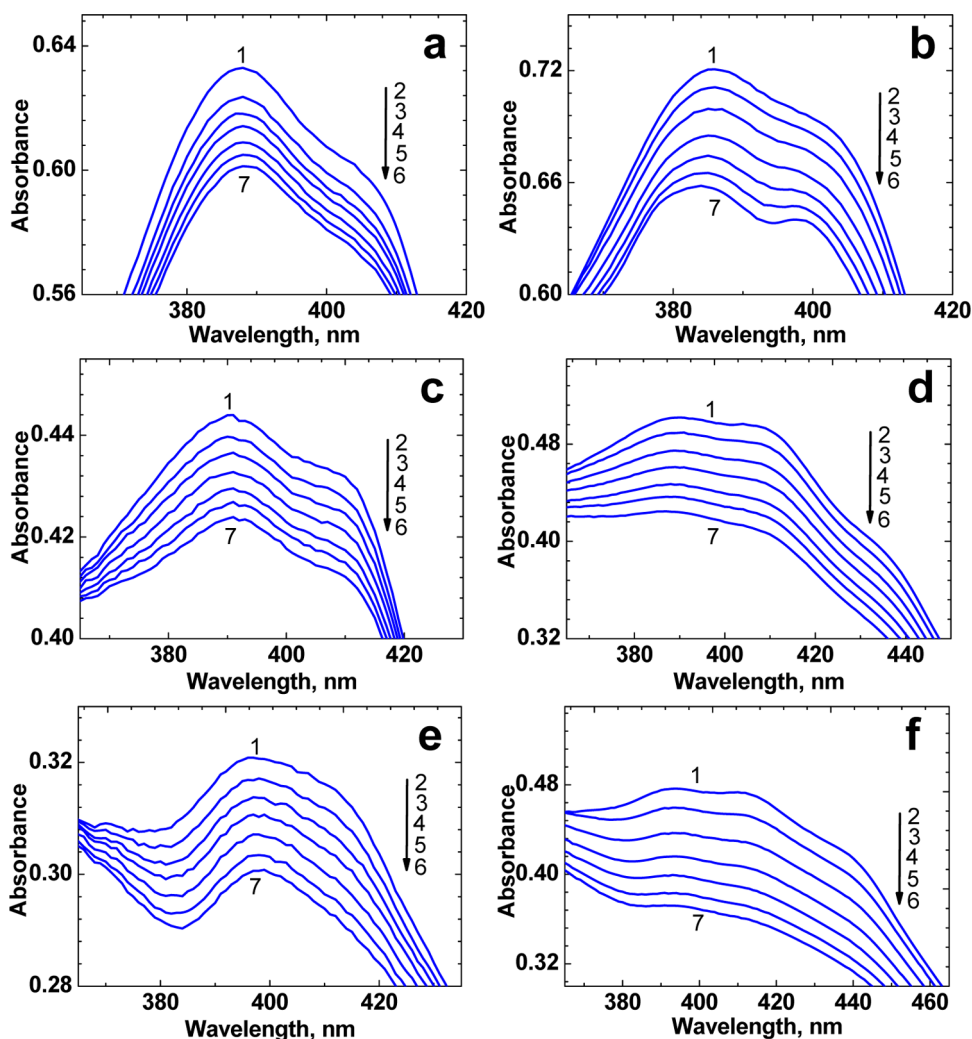


**Figure 5.** Changes in the main IPA band of **1** (a, b), **2** (c, d), and **3** (e, f) in TOL (a, c, e) and DCM (b, d, f) under CW irradiation at 405 nm, with intensity  $I(\lambda_{\text{ex}}) \approx 300 \text{ mW cm}^{-2}$  and corresponding irradiation times,  $t_{\text{ir}} = 0 \text{ min}$  (1), 1–6 min (2–7).

172 component amplitude is incomparably small. The lifetime  
 173 values of the short components are  $\sim 5 \text{ ns}$  and nicely  
 174 correspond to the fluorescence lifetime of the separate TCQ  
 175 molecule in TOL at room temperature.<sup>51</sup> All of the  
 176 experimental data presented above allow us to conclude that  
 177 we simultaneously observe emission from TCQ-based elec-  
 178 tronic levels: fluorescence from the singlet  $^1\text{LC}$  state and  
 179 phosphorescence from the triplet  $^3\text{MLCT}$  state. These two  
 180 emission channels are nearly independent and can be explained  
 181 with a model having a double minima excited-state potential  
 182 surface proposed previously in ref 37. The increase of the long  
 183 lifetime components is in line with the number of iridium  
 184 nuclei in the molecular structure and gives evidence of the  
 185 strong spin–orbit coupling for **1–3**, resulting in the increase in  
 186 triplet population and the corresponding metal-enhanced  
 187 phosphorescence emission. It is worth mentioning that the  
 188 shapes of the steady-state PL spectra (Figure 3) are  
 189 independent of  $\lambda_{\text{ex}}$  in spite of the observed dual-component  
 190 PL emission in the decay kinetic measurements (Figure 4). As  
 191 follows from these decay curves, the integral numbers of  
 192 emission quanta in the observed fluorescence and phosphor-  
 193 escence components are comparable under the pulsed  
 194 picosecond excitation and relatively low repetition rate.  
 195 Nevertheless, taking into account the high singlet–triplet

conversion quantum yields of **1–3**<sup>16</sup> and, as typical for Ir  
 196 complexes, the extremely fast singlet–triplet transformation  
 197 rates ( $\geq 10^{12} \text{ s}^{-1}$ ),<sup>16,22,23</sup> it can be shown from kinetic equations  
 198 that phosphorescence radiation plays a dominant role in the  
 199 steady-state emission spectra. 200

The photochemical stability of **1–3** in air-saturated TOL and  
 201 DCM was estimated using CW laser irradiation at room  
 202 temperature and  $\lambda_{\text{ex}} = 405 \text{ nm}$ . Typical changes in the main  
 203 IPA band are shown in Figure 5. As follows from the data  
 204 analyses, photodecomposition of **1–3** in both solvents can be  
 205 roughly described by first-order photoreactions<sup>55</sup> and no  
 206 substantial evidence of nascent photoproducts were detected  
 207 in the first 7 min of irradiation. The values of the corresponding  
 208 photodecomposition quantum yields  $\Phi_{\text{ph}}$  were determined by  
 209 the absorption method<sup>46</sup> and are presented in Table 1. As  
 210 follows from these data, the highest photostability was observed  
 211 for **2** in nonpolar TOL ( $\Phi_{\text{ph}} \approx 4 \times 10^{-6}$ ). It should be  
 212 mentioned that the photochemical stability of **1–3** was  
 213 practically the same in nonpolar media but noticeably decreased  
 214 in polar DCM in line with the number of iridium nuclei in the  
 215 molecular structure. The values of  $\Phi_{\text{ph}}$  are comparable with the  
 216 corresponding parameters for the best laser dyes<sup>56–58</sup> and  
 217 therefore have potential for practical applications. 218

219 **2PA Spectra of 1–3.** The degenerate 2PA spectra of  
 220 iridium complexes 1–3 were measured in DCM using the  
 221 single-beam Z-scan method<sup>49</sup> with femtosecond excitation and  
 222 are presented in Figure 6. All of these compounds exhibit

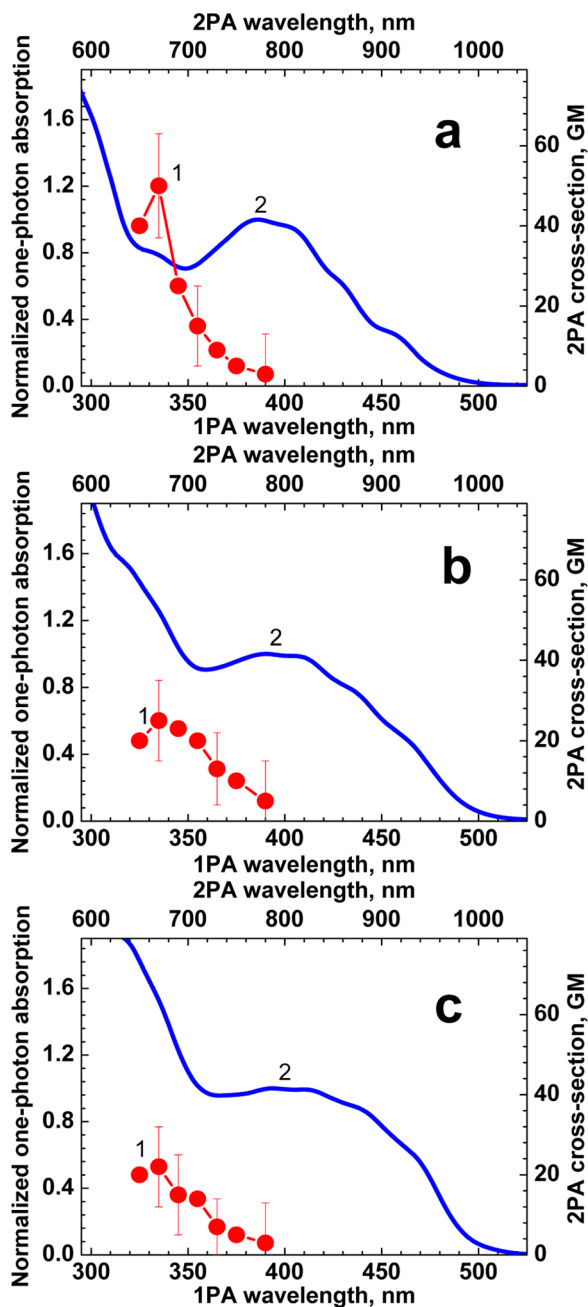


**Figure 6.** Degenerate 2PA (1) and normalized 1PA (2) spectra of 1 (a), 2 (b), and 3 (c) in DCM.

223 maxima 2PA cross sections,  $\delta_{2PA} \approx 25\text{--}50$  GM in the short-  
 224 wavelength region ( $\sim 330\text{--}340$  nm) and dramatically decreased  
 225 values of  $\delta_{2PA}$  in the main long-wavelength absorption band at  
 226  $\sim 390\text{--}400$  nm. Noting the decrease in the 2PA maximum cross  
 227 sections with increasing number of Ir(ppz)<sub>2</sub> units in the  
 228 molecular structure, the dominant role of TCQ-based <sup>1</sup>LC  
 229 singlet transitions in the 2PA properties of 1–3 can be  
 230 assumed. This assumption also agrees with the extremely weak  
 231 linear absorption of the separate TCQ compounds in TOL in  
 232 the spectral range 330–340 nm,<sup>51</sup> where two-photon allowed

transitions can be expected. The noticeably decreased values of  
 $\delta_{2PA}$  in the main linear 1PA band at  $\sim 400$  nm can be explained  
 by the relatively small extinction coefficients and corresponding  
 transition dipoles for TCQ-based  $S_0 \rightarrow {}^1LC$  electronic  
 transitions. This is also in line with the small changes in the  
 corresponding values of the permanent dipoles of 1–3 under  
 these transitions. The last assumption is reasonable due to the  
 weak solvatochromic effect of TCQ at room temperature, as  
 follows from ref 51 where the steady-state fluorescence spectra  
 of this molecule are presented in solvents of different polarities.  
 Typically, an increase in  $\delta_{2PA}$  is correlated with an increase in  
 the number of  $\pi$  electrons in the molecular structure,<sup>59,60</sup> which  
 is obviously not the case for these iridium complexes 1–3,  
 where the reverse tendency is observed in the short-wavelength  
 range. This effect can be explained by the different symmetries  
 of the electronic distributions in the molecular orbitals of TCQ-  
 based <sup>1</sup>LC electronic states in 1–3, where the most  
 asymmetrical configuration having the largest dipolar term in  
 the expression for the 2PA cross section of  $S_0 \rightarrow S_n$  two-photon  
 transition ( $S_n$  is the higher excited electronic state)<sup>61,62</sup> can be  
 expected for 1.

## CONCLUSIONS

Linear photophysics, 2PA, and photochemical stability of  
 multinuclear TCQ-based iridium(III) complexes 1–3 were  
 comprehensively investigated in liquid solutions. Dual-  
 component PL emission was revealed for 1–3 at room  
 temperature and can be assigned to simultaneous observation  
 of fluorescence (short component  $\sim 5$  ns) and phosphorescence  
 (long component  $>150$  ns) from the TCQ-based <sup>1</sup>LC and  
<sup>3</sup>MLCT electronic states, respectively. The amplitudes of the  
 long lifetime components increased with the number of iridium  
 nuclei in the molecular structure. 2PA spectra of 1–3 were  
 measured by a single-beam open aperture Z-scan with 1 kHz  
 femtosecond excitation, and the maximum cross section of  $\sim 50$   
 GM was shown for 1. The nature of 2PA efficiency of 1–3 was  
 mainly determined by the dominant role of the TCQ-based  $S_0$   
 $\rightarrow {}^1LC$  electronic transitions. The photochemical stability of  
 1–3 was investigated under CW irradiation into the main  
 absorption bands and good potential for practical applicability  
 was shown. The highest level of photostability with the  
 corresponding quantum yield of  $\sim 4 \times 10^{-6}$  was obtained for  
 compound 2 in nonpolar TOL solution. The presented dual  
 emission multinuclear Ir complexes exhibiting extremely fast  
 triplet population, high singlet–triplet conversion quantum  
 yields, and significant 2PA with high photochemical stability are  
 of interest for the design of new optoelectronic systems,  
 photodynamic therapy, luminescence sensing, and manifold  
 nonlinear optical applications.

## AUTHOR INFORMATION

### Corresponding Authors

\*E-mail: [mbondar@mail.ucf.edu](mailto:mbondar@mail.ucf.edu). Tel.: 38-044-525-9968 (M.V.B.).

\*E-mail: [ewvs@creol.ucf.edu](mailto:ewvs@creol.ucf.edu). Tel.: 1-407-823-6835 (E.W.V.S.).

### ORCID

Peng Zhao: 0000-0001-6370-4206

Ryan M. O'Donnell: 0000-0002-3565-9783

### Notes

The authors declare no competing financial interest.

## 291 ■ ACKNOWLEDGMENTS

292 E.W.V.S., D.J.H., P.Z., and M.V.B. acknowledge the Army  
293 Research Laboratory (W911NF-15-2-0090) and the National  
294 Science Foundation grant DMR-1609895 for support. P.Z.  
295 acknowledges the UCF Pre-eminent Postdoctoral Program for  
296 funding. M.V.B. wishes to acknowledge the National Academy  
297 of Sciences of Ukraine for funding (grants B-180 and VC/188).

## 298 ■ REFERENCES

299 (1) Liu, D.; Ren, H.; Deng, L.; Zhang, T. Synthesis and  
300 Electrophosphorescence of Iridium Complexes Containing Benzothia-  
301 zole-Based Ligands. *ACS Appl. Mater. Interfaces* **2013**, *5*, 4937–4944.  
302 (2) Martir, D. R.; Momblona, C.; Pertegás, A.; Cordes, D. B.; Slawin,  
303 A. M. Z.; Bolink, H. J.; Zysman-Colman, E. Chiral Iridium(III)  
304 Complexes in Light-Emitting Electrochemical Cells: Exploring the  
305 Impact of Stereochemistry on the Photophysical Properties and Device  
306 Performances. *ACS Appl. Mater. Interfaces* **2016**, *8*, 33907–33915.  
307 (3) Evans, R. C.; Douglas, P.; Winscom, C. J. Coordination  
308 Complexes Exhibiting Room-Temperature Phosphorescence: Evalua-  
309 tion of Their Suitability as Triplet Emitters in Organic Light Emitting  
310 Diodes. *Coord. Chem. Rev.* **2006**, *250*, 2093–2126.  
311 (4) Yersin, H.; Rausch, A. F.; Czerwieńiec, R.; Hofbeck, T.; Fischer,  
312 T. The Triplet State of Organo-Transition Metal Compounds. Triplet  
313 Harvesting and Singlet Harvesting for Efficient OLEDs. *Coord. Chem.*  
314 *Rev.* **2011**, *255*, 2622–2652.  
315 (5) Martí, A. A. Metal Complexes and Time-Resolved Photo-  
316 luminescence Spectroscopy for Sensing Applications. *J. Photochem.*  
317 *Photobiol., A* **2015**, *307–308*, 35–47.  
318 (6) Mei, Q.; Shi, Y.; Chen, C.; Hua, Q.; Tong, B. A Highly Selective  
319 Turn-on Sensor for Hg<sup>2+</sup> Based on a Phosphorescent Iridium (III)  
320 Complex. *Inorg. Chem. Commun.* **2016**, *73*, 147–151.  
321 (7) Xu, W.-J.; Liu, S.-J.; Zhao, X.; Zhao, N.; Liu, Z.-Q.; Xu, H.; Liang,  
322 H.; Zhao, Q.; Yu, X.-Q.; Huang, W. Synthesis, One- and Two-Photon  
323 Photophysical and Excited-State Properties, and Sensing Application  
324 of a New Phosphorescent Dinuclear Cationic Iridium(III) Complex.  
325 *Chem. – Eur. J.* **2013**, *19*, 621–629.  
326 (8) Ma, D.-L.; Zhong, H.-J.; Fu, W.-C.; Chan, D. S.-H.; Kwan, H.-Y.;  
327 Fong, W.-F.; Chung, L.-H.; Wong, C.-Y.; Leung, C.-H. Phosphor-  
328 escent Imaging of Living Cells Using a Cyclometalated Iridium(III)  
329 Complex. *PLoS One* **2013**, *8*, No. e55751.  
330 (9) Yang, H.; Li, L.; Wan, L.; Zhou, Z.; Yang, S. Synthesis of Water  
331 Soluble PEG-Functionalized Iridium Complex Via Click Chemistry  
332 and Application for Cellular Bioimaging. *Inorg. Chem. Commun.* **2010**,  
333 *13*, 1387–1390.  
334 (10) Lee, L. C.-C.; Lau, J. C.-W.; Liu, H.-W.; Lo, K. K.-W. Conferring  
335 Phosphorogenic Properties on Iridium(III)-Based Bioorthogonal  
336 Probes through Modification with a Nitron Unit. *Angew. Chem., Int.*  
337 *Ed.* **2016**, *55*, 1046–1049.  
338 (11) Colombo, A.; Dragonetti, C.; Roberto, D.; Valore, A.; Ferrante,  
339 C.; Fortunati, I.; Picone, A. L.; Todescato, F.; Williams, J. A. G. Two-  
340 Photon Absorption Properties and <sup>1</sup>O<sub>2</sub> Generation Ability of Ir  
341 Complexes: An Unexpected Large Cross Section of [Ir(CO)<sub>2</sub>Cl-(4-  
342 (Para-Di-N-Butylaminostyryl)Pyridine)]. *Dalton Trans.* **2015**, *44*,  
343 15712–15720.  
344 (12) Tian, X.; Zhu, Y.; Zhang, M.; Luo, L.; Wu, J.; Zhou, H.; Guan,  
345 L.; Battaglia, G.; Tian, Y. Localization Matters: A Nuclear Targeting  
346 Two-Photon Absorption Iridium Complex in Photodynamic Therapy.  
347 *Chem. Commun.* **2017**, *53*, 3303–3306.  
348 (13) Wang, L.; Yin, H.; Cui, P.; Hetu, M.; Wang, C.; Monro, S.;  
349 Schaller, R. D.; Cameron, C. G.; Liu, B.; Kilina, S.; McFarland, S. A.;  
350 Sun, W. Near-Infrared-Emitting Heteroleptic Cationic Iridium  
351 Complexes Derived from 2,3-Diphenylbenzo[G]Quinoxaline as *in*  
352 *Vitro* Theranostic Photodynamic Therapy Agents. *Dalton Trans.* **2017**,  
353 *46*, 8091–8103.  
354 (14) Costa, R. D.; Aragón, J.; Ortí, E.; Pappenfus, T. M.; Mann, K. R.;  
355 Matczyszyn, K.; Samoc, M.; Zafra, J. L.; Navarrete, J. T. L.; Casado, J.  
356 Impact of the Synergistic Collaboration of Oligothiophene Bridges and

Ruthenium Complexes on the Optical Properties of Dumbbell-Shaped 357  
Compounds. *Chem. – Eur. J.* **2013**, *19*, 1476–1488. 358  
(15) Shensky, W. M., III; Ferry, M. J.; O'Donnell, R. M.; Ensley, T. 359  
R.; Shi, J. Nonlinear Optical Characterization of Multinuclear Iridium 360  
Compounds Containing Tricycloquinazoline. *Appl. Opt.* **2017**, *56*, 361  
B179–B183. 362  
(16) Four, M.; Riehl, D.; Mongin, O.; Blanchard-Desce, M.; Lawson- 363  
Daku, L. M.; Moreau, J.; Chauvin, J.; Delaire, J. A.; Lemerrier, G. A 364  
Novel Ruthenium(II) Complex for Two-Photon Absorption-Based 365  
Optical Power Limiting in the near-IR Range. *Phys. Chem. Chem. Phys.* 366  
**2011**, *13*, 17304–17312. 367  
(17) Yang, C.; Mehmood, F.; Lam, T. L.; Chan, S. L.-F.; Wu, Y.; 368  
Yeung, C.-S.; Guan, X.; Li, K.; Chung, C. Y.-S.; Zhou, C.-Y.; Zou, T.; 369  
Che, C.-M. Stable Luminescent Iridium(III) Complexes with Bis(N- 370  
Heterocyclic Carbene) Ligands: Photostability, Excited State Proper- 371  
ties, Visible-Lightdriven Radical Cyclization and CO<sub>2</sub> Reduction, and 372  
Cellular Imaging. *Chem. Sci.* **2016**, *7*, 3123–3136. 373  
(18) Pomarico, E.; Silatani, M.; Messina, F.; Braem, O.; Cannizzo, A.; 374  
Barranoff, E.; Klein, J. H.; Lambert, C.; Chergui, M. Dual 375  
Luminescence, Interligand Decay, and Nonradiative Electronic 376  
Relaxation of Cyclometalated Iridium Complexes in Solution. *J.* 377  
*Phys. Chem. C* **2016**, *120*, 16459–16469. 378  
(19) Flamigni, L.; Ventura, B.; Barigelletti, F.; Baranoff, E.; Collin, J.- 379  
P.; Sauvage, J.-P. Luminescent Iridium(III)-Terpyridine Complexes – 380  
Interplay of Ligand Centred and Charge Transfer States. *Eur. J. Inorg.* 381  
*Chem.* **2005**, 1312–1318. 382  
(20) Cross, P. W. C.; Herbert, J. M.; Kerr, W. J.; McNeill, A. H.; 383  
Paterson, L. C. Isotopic Labelling of Functionalised Arenes Catalysed 384  
by Iridium(I) Species of the [(cod)Ir(NHC)(py)]PF<sub>6</sub> Complex Class. 385  
*Synlett* **2016**, *27*, 111–115. 386  
(21) Tang, K.-C.; Liu, K. L.; Chen, I.-C. Rapid Intersystem Crossing 387  
in Highly Phosphorescent Iridium Complexes. *Chem. Phys. Lett.* **2004**, 388  
*386*, 437–441. 389  
(22) Hedley, G. J.; Ruseckas, A.; Samuel, I. D. W. Ultrafast 390  
Intersystem Crossing in a Red Phosphorescent Iridium Complex. *J.* 391  
*Phys. Chem. A* **2009**, *113*, 2–4. 392  
(23) Spaenig, F.; Olivier, J.-H.; Prusakova, V.; Retaillieu, P.; Ziessel, 393  
R.; Castellano, F. N. Excited-State Properties of Heteroleptic 394  
Iridium(III) Complexes Bearing Aromatic Hydrocarbons with 395  
Extended Cores. *Inorg. Chem.* **2011**, *50*, 10859–10871. 396  
(24) Yang, W.; Ashwood, B.; Zhao, J.; Ji, W.; Escudero, D.; 397  
Jacquemin, D.; Crespo-Hernández, C. E. Ultrafast Excited-State 398  
Dynamics in Cyclometalated Ir(III) Complexes Coordinated with 399  
Perylenebisimide and Its  $\pi$ -Radical Anion Ligands. *J. Phys. Chem. C* 400  
**2017**, *121*, 21184–21198. 401  
(25) Lamansky, S.; Djurovich, P.; Murphy, D.; Abdel-Razzaq, F.; Lee, 402  
H.-E.; Adachi, C.; Burrows, P. E.; Forrest, S. R.; Thompson, M. E. 403  
Highly Phosphorescent Bis-Cyclometalated Iridium Complexes: 404  
Synthesis, Photophysical Characterization, and Use in Organic Light 405  
Emitting Diodes. *J. Am. Chem. Soc.* **2001**, *123*, 4304–4312. 406  
(26) Tanaka, I.; Tabata, Y.; Tokito, S. Comparison of Phosphor- 407  
escence Properties of Green-Emitting Ir(ppy)<sub>3</sub> and Red-Emitting 408  
btp<sub>2</sub>Ir(acac). *Jpn. J. Appl. Phys.* **2004**, *43*, L1601–L1603. 409  
(27) Kim, Y.; Park, S.; Lee, Y. H.; Jung, J.; Yoo, S.; Lee, M. H. 410  
Homoleptic Tris-Cyclometalated Iridium Complexes with Substituted 411  
*o*-Cboranes: Green Phosphorescent Emitters for Highly Efficient 412  
Solution-Processed Organic Light-Emitting Diodes. *Inorg. Chem.* **2016**, 413  
*909–917*. 414  
(28) Liu, C.; Yu, H.; Xing, Y.; Gao, Z.; Jin, Z. Photostable Ester- 415  
Substituted Bis-Cyclometalated Cationic Iridium(III) Complexes for 416  
Continuous Monitoring of Oxygen. *Dalton Trans.* **2016**, 734–741. 417  
(29) Chang, W.-L.; Yang, P.-Y. Characterization and Emissive 418  
Property of Microfibers Doped with Fluorine Functionalized Iridium 419  
Complex. *J. Lumin.* **2012**, 403–408. 420  
(30) Tsuboi, T.; Aljaroudi, N. Relaxation Processes in the Triplet 421  
State T<sub>1</sub> of Organic Ir-Compound btp<sub>2</sub>Ir(acac) Doped in PC and CBP 422  
Fluorescent Materials. *J. Lumin.* **2006**, *119–120*, 127–131. 423  
(31) Chew, S.; Lee, C. S.; Lee, S.-T.; Wang, P.; He, J.; Li, W.; Pan, J.; 424  
Zhang, X.; Kwong, H. Photoluminescence and Electroluminescence of 425

- 426 a New Blue-Emitting Homoleptic Iridium Complex. *Appl. Phys. Lett.* 495  
427 **2006**, *88*, No. 093510. 496
- 428 (32) Bezzubov, S. I.; Kiselev, Y. M.; Churakov, A. V.; Kozyukhin, S. 497  
429 A.; Sadovnikov, A. A.; Grinberg, V. A.; Emets, V. V.; Doljenko, V. D. 498  
430 Iridium(III) 2-Phenylbenzimidazole Complexes: Synthesis, Structure, 499  
431 Optical Properties, and Applications in Dye-Sensitized Solar Cells. *Eur.* 500  
432 *J. Inorg. Chem.* **2016**, *2016*, 347–354. 501
- 433 (33) Beeby, A.; Bettington, S.; Samuel, I. D. W.; Wang, Z. Tuning the 502  
434 Emission of Cyclometalated Iridium Complexes by Simple Ligand 503  
435 Modification. *J. Mater. Chem.* **2003**, *13*, 80–83. 504
- 436 (34) Tsuboi, T.; Huang, W. Recent Advances in Multicolor Emission 505  
437 and Color Tuning of Heteroleptic Iridium Complexes. *Isr. J. Chem.* 506  
438 **2014**, *54*, 885–896. 507
- 439 (35) Ho, M.-L.; Lin, M.-H.; Chen, Y.-T.; Sheu, H.-S. Iridium(III) 508  
440 Complexes in Discs for Two-Photon Excitation Applications. *Chem.* 509  
441 *Phys. Lett.* **2011**, *509*, 162–168. 510
- 442 (36) Zhao, P.; Tofighi, S.; O'Donnell, R. M.; Shi, J.; Zavalij, P. Y.; 511  
443 Bondar, M. V.; Hagan, D. J.; Van Stryland, E. W. Electronic Nature of 512  
444 New Ir(III)-Complexes: Linear Spectroscopic and Nonlinear Optical 513  
445 Properties. *J. Phys. Chem. C* **2017**, *121*, 23609–23617. 514
- 446 (37) Chen, Y.; Qiao, L.; Ji, L.; Chao, H. Phosphorescent Iridium(III) 515  
447 Complexes as Multicolor Probes for Specific Mitochondrial Imaging 516  
448 and Tracking. *Biomaterials* **2014**, *35*, 2–13. 517
- 449 (38) Donato, L.; Abel, P.; Zysman-Colman, E. Cationic Iridium(III) 518  
450 Complexes Bearing a Bis(Triazole) Ancillary Ligand. *Dalton Trans.* 519  
451 **2013**, *42*, 8402–8412. 520
- 452 (39) Jin, C.; Liu, J.; Chen, Y.; Guan, R.; Ouyang, C.; Zhu, Y.; Ji, L.; 521  
453 Chao, H. Cyclometalated Iridium(III) Complexes as AIE Phosphor- 522  
454 escent Probes for Real-Time Monitoring of Mitophagy in Living Cells. 523  
455 *Sci. Rep.* **2016**, *6*, No. 22039. 524
- 456 (40) Kim, O.-H.; Ha, S.-W.; Kim, J. I.; Lee, J.-K. Excellent 525  
457 Photostability of Phosphorescent Nanoparticles and Their Application 526  
458 as a Color Converter in Light Emitting Diodes. *ACS Nano* **2010**, *4*, 527  
459 3397–3405. 528
- 460 (41) Belfield, K. D.; Bondar, M. V.; Haniff, H. S.; Mikhailov, I. A.; 529  
461 Luchita, G.; Przhonska, O. V. Superfluorescent Squaraine with 530  
462 Efficient Two-Photon Absorption and High Photostability. *Chem-* 531  
463 *PhysChem* **2013**, *14*, 3532–3542. 532
- 464 (42) Shensky, W. M., III; Shi, J.; Ferry, M. J.; Pritchett, T. M. 533  
465 Tricycloquinazoline-Based Organometallic Compounds for Optical 534  
466 Switching. In *CLEO*, paper SM2G.8; OSA Publishing, 2015. 535
- 467 (43) Lakowicz, J. R. *Principles of Fluorescence Spectroscopy*; Kluwer: 536  
468 New York, 1999. 537
- 469 (44) Mardelli, M.; Olmsted, J. Calorimetric Determination of 9,10- 538  
470 Diphenylanthracene Fluorescence Quantum Yield. *J. Photochem.* **1977**, 539  
471 *7*, 277–285. 540
- 472 (45) Corredor, C. C.; Belfield, K. D.; Bondar, M. V.; Przhonska, O. 541  
473 V.; Yao, S. One- and Two-Photon Photochemical Stability of Linear 542  
474 and Branched Fluorene Derivatives. *J. Photochem. Photobiol., A* **2006**, 543  
475 *184*, 105–112. 544
- 476 (46) Cui, L.-S.; Liu, Y.; Liu, X.-Y.; Jiang, Z.-Q.; Liao, L.-S. Design and 545  
477 Synthesis of Pyrimidine-Based Iridium(III) Complexes with Horizon- 546  
478 tal Orientation for Orange and White Phosphorescent OLEDs. *ACS* 547  
479 *Appl. Mater. Interfaces* **2015**, *7*, 11007–11014. 548
- 480 (47) Liu, T.; Bondar, M. V.; Belfield, K. D.; Anderson, D.; Masunov, 549  
481 A. E.; Hagan, D. J.; Van Stryland, E. W. Linear Photophysics and 550  
482 Femtosecond Nonlinear Spectroscopy of a Star-Shaped Squaraine 551  
483 Derivative with Efficient Two-Photon Absorption. *J. Phys. Chem. C* 552  
484 **2016**, *120*, 11099–11110. 553
- 485 (48) Belfield, K. D.; Bondar, M. V.; Morales, A. R.; Yue, X.; Luchita, 554  
486 G.; Przhonska, O. V. Transient Excited-State Absorption and Gain 555  
487 Spectroscopy of a Two-Photon Absorbing Probe with Efficient 556  
488 Superfluorescent Properties. *J. Phys. Chem. C* **2012**, *116*, 11261– 557  
489 11271. 558
- 490 (49) Sheik-Bahae, M.; Said, A. A.; Wei, T.-H.; Hagan, D. J.; Van 559  
491 Stryland, E. W. Sensitive Measurement of Optical Nonlinearities Using 560  
492 a Single Beam. *IEEE J. Quantum Electron.* **1990**, *26*, 760–769. 561
- 493 (50) Padilha, L. A.; Webster, S.; Przhonska, O. V.; Hu, H.; Peceli, D.; 562  
494 Rosch, J. L.; Bondar, M. V.; Gerasov, A. O.; Kovtun, Y. P.; Shandura, 563  
495 M. P.; Kachkovski, A. D.; Hagan, D. J.; Van Stryland, E. W. Nonlinear 564  
496 Absorption in a Series of Donor– $\pi$ –Acceptor Cyanines with Different 565  
497 Conjugation Lengths. *J. Mater. Chem.* **2009**, *19*, 7503–7513. 566
- (51) Cundall, R. B.; Grant, D. J. W.; Shulman, N. H. Photophysics of 567  
5,10,14c,15-Tetra-Azabenz[*a*]Naphth[1,2,3-*de*]Anthracene (Tricyclo- 568  
quinazoline, TCQ) and Some of Its Derivatives. *J. Chem. Soc., Faraday* 569  
*Trans. 2* **1982**, *78*, 737–750. 570
- (52) Cundall, R. B.; Grant, D. J. W.; Shulman, N. H. Photophysics of 571  
4a,5,10,15-Tetra-Azabenz[*a*]Naphth[1,2,3-*de*]Anthracene (NTCQ, 572  
the Ring-Nitrogen Isostere of Tricycloquinazoline). *J. Chem. Soc.,* 573  
*Faraday Trans. 2* **1982**, *78*, 27–37. 574
- (53) Howarth, A. J.; Majewski, M. B.; Brown, C. M.; Lelj, F.; Wolf, 575  
M. O.; Patrick, B. O. Emissive Ir(III) Complexes Bearing 576  
Thienylamido Groups on a 1,10-Phenanthroline Scaffold. *Dalton* 577  
*Trans.* **2015**, *44*, 16272–16279. 578
- (54) Sunesh, C. D.; Choe, Y. Synthesis and Characterization of 579  
510 Cationic Iridium Complexes for the Fabrication of Green and Yellow 580  
511 Light-Emitting Devices. *Mater. Chem. Phys.* **2015**, *156*, 206–213. 581
- (55) Ollis, D.; Mills, A.; Lawrie, K. Kinetics of Methylene Blue (MB) 582  
514 Photocatalyzed Reduction and Dark Regeneration in a Colorimetric 583  
515 Oxygen Sensor. *Appl. Catal., B* **2016**, *184*, 201–207. 584
- (56) El-Daly, S. A.; El-Azim, S. A.; Elmekawey, F. M.; Elbaradei, B. 585  
516 Y.; Shama, S. A.; Asiri, A. M. Photophysical Parameters, Excitation 586  
517 Energy Transfer, and Photoreactivity of 1,4-Bis(5-Phenyl-2-Oxazolyl)- 587  
518 Benzene (POPOP) Laser Dye. *Int. J. Photoenergy* **2012**, *2012*, 588  
519 No. 458126. 589
- (57) Rosenthal, I. Photochemical Stability of Rhodamine 6G in 590  
521 Solution. *Opt. Commun.* **1978**, *24*, 164–166. 591
- (58) Azim, S. A.; Al-Hazmy, S. M.; Ebeid, E. M.; El-Daly, S. A. A New 592  
523 Coumarin Laser Dye 3-(Benzothiazol-2-yl)-7-Hydroxycoumarin. *Opt.* 593  
524 *Laser Technol.* **2005**, *37*, 245–249. 594
- (59) Kuzyk, M. G. Fundamental Limits on Two-Photon Absorption 595  
526 Cross Sections. *J. Chem. Phys.* **2003**, *119*, 8327–8335. 596
- (60) Moreno, J. P.; Kuzyk, M. G. Fundamental Limits of the 597  
528 Dispersion of the Two-Photon Absorption Cross Section. *J. Chem.* 598  
529 *Phys.* **2005**, *123*, No. 194101. 599
- (61) Orr, B. J.; Ward, J. F. Perturbation Theory of Non-Linear 600  
531 Optical Polarization of an Isolated System. *Mol. Phys.* **1971**, *20*, 513– 601  
532 526. 602
- (62) Ohta, K.; Antonov, L.; Yamada, S.; Kamada, K. Theoretical 603  
534 Study of the Two-Photon Absorption Properties of Several Asym- 604  
535 metrically Substituted Stilbenoid Molecules. *J. Chem. Phys.* **2007**, *127*, 605  
536 No. 084504. 606